Entanglement duality in spin-spin interactions

Vahid Azimi-Mousolou,[1,2,*] Anders Bergman,[2] Anna Delin,[3,4] Olle Eriksson,[2,5] Manuel Pereiro,[2] Danny Thonig,[5,2] and Erik Sjöqvist[2,†]

[1]*Department of Applied Mathematics and Computer Science, Faculty of Mathematics and Statistics, University of Isfahan, Isfahan 81746-73441, Iran*

[2]*Department of Physics and Astronomy, Uppsala University, Box 516, SE-751 20 Uppsala, Sweden*

[3]*Department of Applied Physics, School of Engineering Sciences, KTH Royal Institute of Technology, AlbaNova University Center, SE-10691 Stockholm, Sweden*

[4]*Swedish e-Science Research Center (SeRC), KTH Royal Institute of Technology, SE-10044 Stockholm, Sweden*

[5]*School of Science and Technology, Örebro University, SE-701 82 Örebro, Sweden*

(Received 6 May 2022; accepted 25 August 2022; published 6 September 2022)

We examine entanglement of thermal states for spin-1/2 dimers in external magnetic fields. Entanglement transition in the temperature-magnetic-field plane demonstrates a duality in spin-spin interactions. This identifies a pair of dual categories of symmetric and antisymmetric dimers with each category classified into toric entanglement classes. The entanglement transition line is preserved from each toric entanglement class to its dual toric class. The toric classification is an indication of the topological signature of the entanglement, which bring about topological stability that could be relevant for quantum information processing.

DOI: 10.1103/PhysRevA.106.032407

I. INTRODUCTION

The classification concept has been incorporated in different scientific fields, ranging from biological systems to abstract topology in mathematics in order to categorize relevant objects based on shared characteristics. Scientific classification schemes have not only led to new discoveries of materials and resources, such as in the topological classification of matter [1] and of entangled quantum states [2], but have also helped significantly to find the most efficient and robust approaches to technological advances.

One of the fundamental characteristics of quantum mechanics is the quantum entanglement, which lies at the heart of the difference between the classical and the quantum worlds [3–5]. It is widely believed to be stronger than classical correlations and over the years has become a critically important resource for many applications in quantum technology, including quantum computing, quantum cryptography, quantum communication, and hypersensitive measurements [6]. As a primary attribute of quantum mechanics, quantum entanglement is also much more involved with the foundations, predictions, and interpretations of quantum phenomena. It is strongly linked to the concepts of quantum phase transition and quantum geometric phases [7–12]. Despite significant works having been published, the characteristics of the quantum entanglement is far from a closed topic. New in-depth investigations of existing or entirely new models or systems, continue to enrich this field and to add to the understanding of quantum phenomena, in general.

Here we use entanglement in terms of concurrence [13,14] from a classification perspective in order to analyze spin-spin interactions in atomic dimers and to classify them into entanglement classes. To this end, we focus on the entanglement transition line for thermal states of a generic traceless spin-pair model in the external parameter space specified by temperature (T) and applied magnetic-field (B). We classify the system into a pair of dual categories of symmetric and antisymmetric dimers. Each category consists of toric entanglement classes where each class and its dual are distinguished by the same entanglement transition line on the T-B plane. As a nontrivial example, we introduce dual symmetric and antisymmetric Heisenberg spin-pair interactions and specify their toric entanglement classes. We note that in Ref. [15], the entanglement between two spins in a one-dimensional Heisenberg chain has been studied as a function of temperature and external magnetic field, but not from the classification approach, which is the main focus here. We also note here that the chosen system, the dimer, is not only an excellent model system, it also has real physical relevance since atomic clusters of any size or shape can be realized experimentally, e.g., as ad-atoms on a substrate [16].

II. GENERAL MODEL HAMILTONIAN

We start with a generic traceless spin-pair model described by the Hamiltonian (note that we use $\hbar = 1$ throughout the

*v.azimi@sci.ui.ac.ir
†erik.sjoqvist@physics.uu.se

paper),

$$H(\omega, \mathbb{J}) = \frac{B_+}{2} s_z^{(1)} + \frac{B_-}{2} s_z^{(2)} + \boldsymbol{s}^{(1)} \cdot \mathbb{J} \boldsymbol{s}^{(2)}, \tag{1}$$

with $\boldsymbol{s}^{(n)} = (s_x^{(n)}, s_y^{(n)}, s_z^{(n)})$ being the spin vector operator acting on spins at site $n = 1, 2$ of the dimer. We also have that

$$\mathbb{J} = \begin{pmatrix} J_{xx} & J_{xy} & 0 \\ J_{yx} & J_{yy} & 0 \\ 0 & 0 & J_{zz} \end{pmatrix}, \tag{2}$$

which is a real-valued matrix describing the essential exchange interactions between the two spins. The matrix elements of this matrix are as follows:

$$\begin{aligned} &J_{xx} = J + r, \qquad J_{yy} = J - r, \\ &J_{xy} = K - D, \qquad J_{yx} = K + D, \\ &B_\pm = \omega \pm \Delta. \end{aligned} \tag{3}$$

This model accounts for a wide range of important spin-spin interaction systems, including the Heisenberg interaction ($J_{zz} = J$), the Dzyaloshinskii-Moriya (D) interaction, the symmetric anisotropic exchange (K), as well as anisotropy of the exchange on the XY plane (r). It further allows for the spins to interact differently with the external magetic-field ($B_\pm$), due to field inhomogenties. From a physical point of view this would best be performed by studies of magnetic dimers as ad-atoms on an overlayer with heterogeneous magnetic structure, or by investigations of dimers with different magnetization direction for the two sites.

The two-qubit Hamiltonian [corresponding to $s_z = \pm 1/2$ in Eq. (1)] is chosen so as to ensure that the thermal equilibrium state at temperature T is of the X type, i.e.,

$$\varrho_T = \frac{1}{\mathcal{Z}} e^{-H/T} = \begin{pmatrix} \rho_{11} & 0 & 0 & \rho_{14} \\ 0 & \rho_{22} & \rho_{23} & 0 \\ 0 & \rho_{32} & \rho_{33} & 0 \\ \rho_{41} & 0 & 0 & \rho_{44} \end{pmatrix}, \tag{4}$$

in the ordered product qubit-qubit basis $\{|00\rangle, |01\rangle, |10\rangle, |11\rangle\}$ and Boltzmann's constant is absorbed in T. Explicitly, we have

$$\begin{aligned} \rho_{11} &= \frac{1}{\mathcal{Z}} e^{-(J_{zz}/4T)} \Big[\cosh \frac{\epsilon_1}{2T} - \sinh \frac{\epsilon_1}{2T} \cos \vartheta \Big], \\ \rho_{44} &= \frac{1}{\mathcal{Z}} e^{-(J_{zz}/4T)} \Big[\cosh \frac{\epsilon_1}{2T} + \sinh \frac{\epsilon_1}{2T} \cos \vartheta \Big], \\ \rho_{14} &= \rho_{41}^* = -\frac{1}{\mathcal{Z}} e^{-(J_{zz}/4T)} e^{-i\varphi} \sinh \frac{\epsilon_1}{2T} \sin \vartheta, \\ \rho_{22} &= \frac{1}{\mathcal{Z}} e^{J_{zz}/4T} \Big[\cosh \frac{\epsilon_2}{2T} - \sinh \frac{\epsilon_2}{2T} \cos \theta \Big], \\ \rho_{33} &= \frac{1}{\mathcal{Z}} e^{J_{zz}/4T} \Big[\cosh \frac{\epsilon_2}{2T} + \sinh \frac{\epsilon_2}{2T} \cos \theta \Big], \\ \rho_{23} &= \rho_{32}^* = -\frac{1}{\mathcal{Z}} e^{J_{zz}/4T} e^{-i\phi} \sinh \frac{\epsilon_2}{2T} \sin \theta, \end{aligned} \tag{5}$$

where

$$\tan \vartheta = \frac{\sqrt{r^2 + K^2}}{\omega}, \qquad \tan \varphi = \frac{K}{r},$$

$$\tan \theta = \frac{\sqrt{J^2 + D^2}}{\Delta}, \qquad \tan \phi = \frac{D}{J}, \tag{6}$$

$$\epsilon_1 = \sqrt{\omega^2 + r^2 + K^2}, \qquad \epsilon_2 = \sqrt{\Delta^2 + J^2 + D^2},$$

and $\mathcal{Z} = 2(e^{-(J_{zz}/4T)} \cosh \frac{\epsilon_1}{2T} + e^{J_{zz}/4T} \cosh \frac{\epsilon_2}{2T})$ the partition function.

The above X-state form is suitable in our analysis for two reasons: (i) as pointed out before, it accounts for thermal states of several important spin-spin interaction models, and (ii) the entanglement measure concurrence $C(\varrho_T)$ [13,14] can be calculated analytically. Indeed, one finds [17]

$$C(\varrho_T) = 2 \max\{C_1, C_2, 0\}, \tag{7}$$

where

$$\begin{aligned} C_1 &= |\rho_{14}| - \sqrt{\rho_{22}\rho_{33}}, \\ C_2 &= |\rho_{23}| - \sqrt{\rho_{11}\rho_{44}}. \end{aligned} \tag{8}$$

We continue the analysis by exploring the entanglement transition for which one may solve

$$\max\{C_1, C_2\} = 0, \tag{9}$$

to extract the critical line in the temperature-magnetic-field parameter space. Equation (9) gives rise to the following duality:

$$\begin{aligned} &\text{(I)} \quad C_2 \leqslant C_1 = 0, \\ &\text{(II)} \quad C_1 \leqslant C_2 = 0, \end{aligned} \tag{10}$$

which becomes

$$\begin{aligned} &\text{(I)} \quad e^{-(J_{zz}/2T)} p^2 - e^{J_{zz}/2T} q^2 = e^{2J_{zz}/T}, \\ &\text{(II)} \quad e^{J_{zz}/2T} q^2 - e^{-(J_{zz}/2T)} p^2 = e^{-(2J_{zz}/T)} \end{aligned} \tag{11}$$

for our model system with $p = f(\epsilon_1, \nu)$ and $q = f(\epsilon_2, \theta)$ given by the function $f(x, y) = \sinh \frac{x}{2T} \sin y$.

This duality relation allows us to categorize the spin-spin interactions in dimers into a pair of dual categories of interactions. We continue by focusing on symmetric and antisymmetric dimers in the sense that the two spins of same magnitude forming the dimer are either parallel and antiparallel. For each case the corresponding Hamiltonian has the following form:

(1) *Symmetric case*. For parallel magnetic moments we would in the simples case have $\Delta = 0$ and $B_+ = B_- = \omega$. Therefore, interactions of symmetric dimers can be described by the following Hamiltonian:

$$\begin{aligned} H_{\rm s} = \frac{B}{2} \big[s_z^{(1)} + s_z^{(2)} \big] &+ J_{zz} s_z^{(1)} s_z^{(2)} \\ &+ J \big[s_x^{(1)} s_x^{(2)} + s_y^{(1)} s_y^{(2)} \big] - D \big[s_x^{(1)} s_y^{(2)} - s_y^{(1)} s_x^{(2)} \big] \\ &+ r \big[s_x^{(1)} s_x^{(2)} - s_y^{(1)} s_y^{(2)} \big] + K \big[s_x^{(1)} s_y^{(2)} + s_y^{(1)} s_x^{(2)} \big]. \end{aligned} \tag{12}$$

Note that $\Delta = 0$ implies $\theta = \pi/2$.

(2) *Antisymmetric case*. In the case of antiparallel magnetic moments, we would in the simplest form have $\omega = 0$ and $B_+ = -B_- = \Delta$, the interactions of antisymmetric dimers

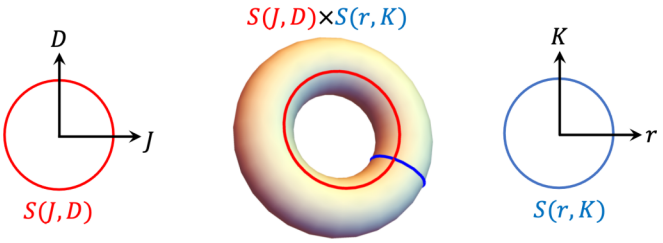

FIG. 1. Schematic of an S class or AS class as a two-dimensional torus in the (J, D, r, K) parameter space.

can be described by

$$H_s = \frac{B}{2}\left[s_z^{(1)} - s_z^{(2)}\right] - J_{zz}s_z^{(1)}s_z^{(2)} + J\left[s_x^{(1)}s_x^{(2)} + s_y^{(1)}s_y^{(2)}\right] - D\left[s_x^{(1)}s_y^{(2)} - s_y^{(1)}s_x^{(2)}\right] + r\left[s_x^{(1)}s_x^{(2)} - s_y^{(1)}s_y^{(2)}\right] + K\left[s_x^{(1)}s_y^{(2)} + s_y^{(1)}s_x^{(2)}\right]. \quad (13)$$

In contrast to symmetric dimers, here we have $\nu = \pi/2$ as a result of $\omega = 0$.

Besides the differences, these two categories share the last two lines in their Hamiltonians.

We note that (I) and (II) in Eq. (11) classify each of the above categories into equivalence classes of dimers within that category in a way that all the dimers in the same class have the same entanglement phase diagram in the T-B parameter space. That is, each class obeys a single critical line on the T-B plane, across which the corresponding thermal states change their entanglement feature from entangled to separable, and vice versa. Explicitly, if we solve Eq. (11) for the critical line on the T-B plane, we find that two dimers specified with interaction parameters (J, D, r, K) and (J', D', r', K) give rise to the same critical line on the T-B plane or they are in the same class if and only if,

$$J^2 + D^2 = J'^2 + D'^2,$$
$$r^2 + K^2 = r'^2 + K'^2. \quad (14)$$

In other words, the above symmetric and antisymmetric categories consist of equivalence classes of dimers where each class can be represented topologically as a two-dimensional torus in the (J, D, r, K) parameter space as shown in Fig. 1. Here, we may refer to an equivalence class of symmetric dimers as an S class and an equivalence class of antisymmetric dimers as an AS class.

Having each category of dimers classified into equivalent toric classes of entangled spins, we further note that each class in one category has its one-to-one corresponding dual class in the opposite category. To see this we observe that the two equations in the duality equation Eq. (12) are related by flipping the sign of the J_{zz}-coupling parameter and exchanging the p and q functions. Therefore, if a given toric S class characterized by the coupling parameters (J, D, r, K) is obtained by one of the equations in Eq. (12), then its corresponding dual AS class characterized by the coupling parameters $(\tilde{J}, \tilde{D}, \tilde{r}, \tilde{K})$ can be obtained from the other equation in Eq. (12) and vice versa. The two dual toric S and AS classes are equivalent in the sense that they give rise to the same entanglement phase diagram on the T-B plane if their characterization parameters

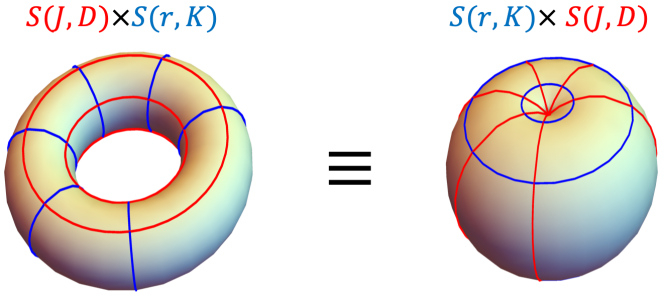

FIG. 2. Toric visualization of dual symmetric and antisymmetric entanglement classes. Each class has the same toric characteristic as its dual but with longitudinal or meridian circles in swapped order.

satisfy the following relations:

$$J^2 + D^2 = \tilde{r}^2 + \tilde{K}^2,$$
$$r^2 + K^2 = \tilde{J}^2 + \tilde{D}^2. \quad (15)$$

These relations compared to the ones given in Eq. (15) indicate that the dual symmetric and antisymmetric entanglement classes have the same toric characteristic but with their longitudinal or meridian circles in swapped order as depicted in Fig. 2.

Although the above analysis focuses on concurrence, it is generally independent of the quantum entanglement measure as it is mainly based on the entanglement transition line on the T-B plane. For instance, one can obtain exactly the same classification and entanglement duality using nonlocality [18,19] and negativity [20]. Note that similar to nonlocality, negativity does not, in general, share the same features with concurrence [21,22]. Other than the entanglement duality, our analysis establishes the topological signature of quantum entanglement in a sense that the entanglement phase diagram in dimers provides a clear topological foliation of the coupling parameters manifold into two-dimensional compact torus leaves [23]. Moreover, the toric classifications given in Eqs. (15) and (16) verify that any sets of coupling parameters on the equivalent dual tori give rise to the same entanglement transition line and indeed the same entanglement region on the T-B plane. In other words, as long as the coupling parameters change within the dual tori specified by Eqs. (15) and (16) the entanglement characteristics of the thermal state remain invariant on the T-B plane. This implies a topological stability, namely, robustness of the entanglement in spin-1/2 dimers against variations of the coupling parameters in larger topological domain.

To further clarify our point and show that the entanglement analysis above provides a nontrivial classification and duality, we consider two examples in the following section.

III. EXAMPLES

Consider two identical spin-1/2 particles with Heisenberg spin-spin exchange interaction of strength J in an external magnetic field as given by the Hamiltonian,

$$H^{\mathrm{HE}} = \frac{B}{2}\left[s_z^{(1)} + s_z^{(2)}\right] + J\mathbf{s}^{(1)} \cdot \mathbf{s}^{(2)}. \quad (16)$$

Note that we use superscript HE here to indicate a Hamiltonian of pure Heisenberg form. In the analysis that follows, we

consider antiferromagnetic coupling $J > 0$ as entanglement cannot occur for ferromagnetic coupling [15]. According to the above classification, the Heisenberg model belongs to a class of symmetric dimers described by the following general form of the Hamiltonian,

$$H_{\rm s}^{\rm HE} = \frac{B}{2}\left[s_z^{(1)} + s_z^{(2)}\right] + J s_z^{(1)} s_z^{(2)} + J'\left[s_x^{(1)} s_x^{(2)} + s_y^{(1)} s_y^{(2)}\right] - D'\left[s_x^{(1)} s_y^{(2)} - s_y^{(1)} s_x^{(2)}\right], \tag{17}$$

such that

$$J'^2 + D'^2 = J^2. \tag{18}$$

Note that $H_{\rm s}^{\rm HE} = H^{\rm HE}$ for $D' = 0$ and $J' = J$. This accompanies the dual-antisymmetric Heisenberg model described by the Hamiltonian,

$$H_{\rm as}^{\rm HE} = \frac{B}{2}\left[s_z^{(1)} - s_z^{(2)}\right] - J s_z^{(1)} s_z^{(2)} + \tilde{r}\left[s_x^{(1)} s_x^{(2)} - s_y^{(1)} s_y^{(2)}\right] + \tilde{K}\left[s_x^{(1)} s_y^{(2)} + s_y^{(1)} s_x^{(2)}\right], \tag{19}$$

where

$$\tilde{r}^2 + \tilde{K}^2 = J^2, \tag{20}$$

with J being the Heisenberg coupling constant in Eq. (16).

By applying the general formulation of the former section to Heisenberg classes, we obtain the following concurrence functions for the corresponding thermal states,

$$C_{\rm s;1}^{\rm HE} = -\frac{(1 + e^{J/T})}{2\mathcal{Z}} < 0,$$
$$C_{\rm s;2}^{\rm HE} = \frac{e^{J/T} - 3}{2\mathcal{Z}}, \tag{21}$$

and

$$C_{\rm as;1}^{\rm HE} = \frac{e^{J/T} - 3}{2\mathcal{Z}},$$
$$C_{\rm as;2}^{\rm HE} = -\frac{(1 + e^{J/T})}{2\mathcal{Z}} < 0, \tag{22}$$

with partition function,

$$\mathcal{Z} = 1 + e^{J/T} + 2\cosh(B/2T). \tag{23}$$

Here we have used the conditions in Eqs. (18) and (20) in the derivations of Eqs. (22)–(23). Note that the swap of the antisymmetric concurrence functions in Eq. (23) compared to its symmetric counterparts in Eq. (22) is what explains the entanglement duality in Heisenberg spin-spin interactions. This duality is associated with coinciding entanglement concurrences,

$$C\left(\varrho_{T;\rm s}^{\rm HE}\right) = \max\left\{\frac{e^{J/T} - 3}{\mathcal{Z}'}, 0\right\} = C\left(\varrho_{T;\rm as}^{\rm HE}\right), \tag{24}$$

for both symmetric and antisymmetric Heisenberg thermal states. Equation (24) defines the critical temperature (that is independent of the external magnetic field),

$$T_c^{\rm HE} = \sqrt{J'^2 + D'^2}/\ln 3 = J/\ln 3 \approx 0.91J, \tag{25}$$

above which as shown in Fig. 3, the thermal states $\varrho_{T;\rm s}^{\rm HE}$ and $\varrho_{T;\rm as}^{\rm HE}$ cease to be entangled. The same critical temperature has been obtained in Ref. [15] for antiferromagnetic Heisenberg model given in Eq. (16). Nonetheless, our analysis shows that this critical temperature indeed holds for a wider class of spin-spin interactions.

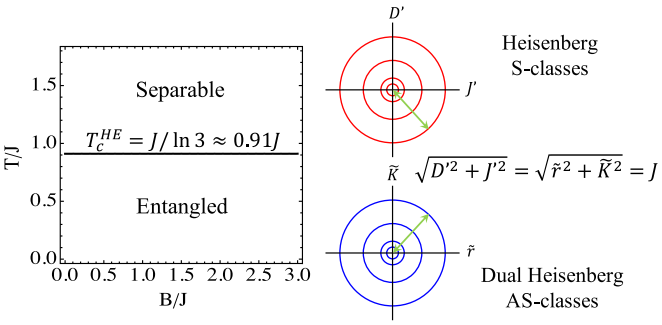

FIG. 3. The left panel shows the entanglement phase diagram for symmetric and dual-antisymmetric Heisenberg dimers on the T-B plane. For each of the Heisenberg-type dimers, the entanglement undergoes a sudden change at the relative critical temperature $T_c^{\rm HE} = J/\ln 3 \approx 0.91J$ independent of the applied magnetic-field strength B. This is an indication of a quantum phase transition. The right panels illustrate toric visualization of the symmetric (S) and antisymmetric (AS) Heisenberg entanglement classes. Whereas each circle of radius J on the (J', D') plane represents a Heisenberg S class corresponding to a given isotropic Heisenberg exchange coupling J, the equivalent dual AS class is represented by a circle on the $(\tilde{r}, \tilde{K})$ plane with the same radius of J.

The entanglement duality for the Heisenberg interaction is identified mainly by the toric characteristic equations given in Eqs. (18) and (20). As illustrated in Fig. 3, these equations foliate the corresponding dual parameter spaces (J', D') and $(\tilde{r}, \tilde{K})$ into circles of radii specified by the Heisenberg exchange parameter J. Each radius identifies dual circles representing dual-symmetric and -antisymmetric classes associated with the Heisenberg spin-spin interaction. Moreover, all spin-spin interaction Hamiltonians in given dual topological classes obey the same critical temperature, given in Eq. (25).

As another example, Fig. 4 illustrates the classification of the XY interaction described by the Hamiltonian,

$$H^{\rm XY} = (1 + r)s_x^{(1)} s_x^{(2)} + (1 - r)s_y^{(1)} s_y^{(2)} + \frac{B}{2}\left[s_z^{(1)} + s_z^{(2)}\right] \tag{26}$$

(with superscript XY) into dual toric entanglement classes. Here $r \in [0, 1]$ is the anisotropy parameter controlling the cylindrical asymmetry of the spin-spin interaction. The XY model given in Eq. (26) defines interactions from the isotropic limit $r = 0$ with additional symmetry $[H^{\rm XY}, s^z] = 0$ to the opposite limit $r = 1$, which corresponds to the Ising type of interactions.

The XY interaction given in Eq. (26) represents a symmetric class of dimers. Following Eqs. (12) and (13), the associated general symmetric and dual-antisymmetric

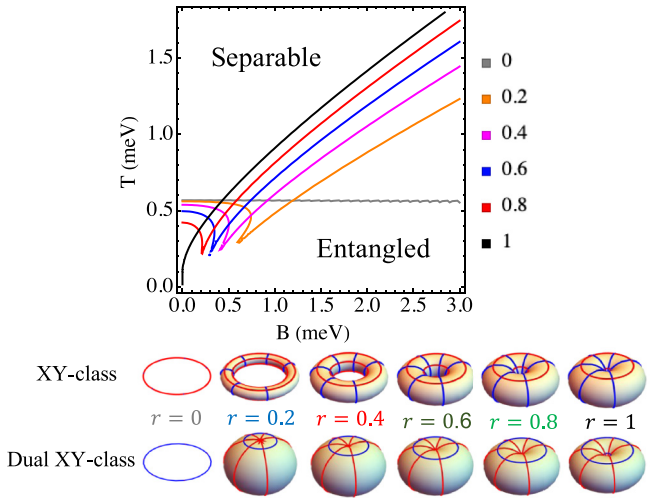

FIG. 4. The upper panel shows the entanglement transition curve for symmetric and dual-antisymmetric XY dimers for different values of anisotropy parameter r. Whereas the isotropic limit $r = 0$ represents the narrowest area of entanglement with magnetic field independent critical temperature, the critical temperature becomes magnetic-field dependent for $r \neq 0$ and the entanglement area monotonically increases with r so that the Ising limit $r = 1$ represents the broadest entanglement area on the T-B plane. Each value of r distinguishes a pair of symmetric and dual-antisymmetric toric entanglement classes depicted in the lower panel.

Hamiltonians read

$$H_{\rm s}^{\rm XY} = \frac{B}{2}\left[s_z^{(1)} + s_z^{(2)}\right] + J'\left[s_x^{(1)}s_x^{(2)} + s_y^{(1)}s_y^{(2)}\right] - D'\left[s_x^{(1)}s_y^{(2)} - s_y^{(1)}s_x^{(2)}\right] + r'\left[s_x^{(1)}s_x^{(2)} - s_y^{(1)}s_y^{(2)}\right] + K'\left[s_x^{(1)}s_y^{(2)} + s_y^{(1)}s_x^{(2)}\right], \tag{27}$$

and

$$H_{\rm as}^{\rm XY} = \frac{B}{2}\left[s_z^{(1)} - s_z^{(2)}\right] + \tilde{J}\left[s_x^{(1)}s_x^{(2)} + s_y^{(1)}s_y^{(2)}\right] - \tilde{D}\left[s_x^{(1)}s_y^{(2)} - s_y^{(1)}s_x^{(2)}\right] + \tilde{r}\left[s_x^{(1)}s_x^{(2)} - s_y^{(1)}s_y^{(2)}\right] + \tilde{K}\left[s_x^{(1)}s_y^{(2)} + s_y^{(1)}s_x^{(2)}\right], \tag{28}$$

with equivalent toric characteristic equations,

$$J'^2 + D'^2 = 1, \quad r'^2 + K'^2 = r^2 \equiv \tilde{J}^2 + \tilde{D}^2 = r^2 \quad \tilde{r}^2 + \tilde{K}^2 = 1. \tag{29}$$

One may note that $H_{\rm s}^{\rm XY} = H^{\rm XY}$ when $J' = 1$ and $r' = r$. For each value of r Eq. (30) specifies a pair of dual toric XY entanglement classes as depicted in the lower panel of Fig. 4. In fact, it is the anisotropy parameter r that controls the entanglement classes and the spin-spin duality.

We obtain the following concurrence functions for the XY classes of thermal states,

$$C_{\rm s;1}^{\rm XY} = \frac{1}{\mathcal{Z}}\left[\frac{r\,\sinh\left(\frac{\sqrt{B^2+r^2}}{2T}\right)}{\sqrt{B^2+r^2}} - \cosh\left(\frac{1}{2T}\right)\right] = C_{\rm as;2}^{\rm XY},$$

$$C_{\rm s;2}^{\rm XY} = \frac{1}{\mathcal{Z}}\left[\sinh\left(\frac{1}{2T}\right) - \sqrt{1 + \frac{r^2\sinh^2\left(\frac{\sqrt{B^2+r^2}}{2T}\right)}{B^2+r^2}}\right] = C_{\rm as;1}^{\rm XY}, \tag{30}$$

with partition function $\mathcal{Z} = 2\cosh(\frac{1}{2T}) + 2\cosh(\frac{\sqrt{B^2+r^2}}{2T})$. For all $r \neq 0$, Eq. (31) derives a magnetic-field-dependent critical temperature given implicitly by

$$\max\left(C_{\rm s;1}^{\rm XY}, C_{\rm s;2}^{\rm XY}\right) = \max\left(C_{\rm as;1}^{\rm XY}, C_{\rm as;2}^{\rm XY}\right) = 0. \tag{31}$$

Figure 4 illustrates critical temperatures as functions of the magnetic field for some values of r.

IV. CONCLUSIONS

In conclusion, we have demonstrated an entanglement duality in a wide class of physically important spin-spin interaction dimer models. This is performed by analyzing an entanglement transition of thermal states on the temperature-magnetic-field plane. The entanglement analysis allows to foliate the coupling parameter space into a dual-pair of symmetric and antisymmetric toric entanglement classes. This classification is an indication of the topological signature of quantum entanglement in the sense that quantum entanglement is consistent up to topological classifications. The analysis shows the stability of entanglement against parameter changes within a broader topological domain, which could be relevant for the processing of quantum information. We hope the present results can contribute to a deeper understanding of the hidden aspects of the concept of quantum entanglement, and that it is an inspiration to works in nanomagnetism where magnetic nanosized objects of the type investigated here are under focus.

ACKNOWLEDGMENTS

We acknowledge financial support from the Knut and Alice Wallenberg Foundation through Grant No. 2018.0060. A.B. and O.E. acknowledge eSSENCE. A.D. acknowledges financial support from the Swedish Research Council (VR) through Grants No. 2019-05304 and No. 2016-05980. O.E. acknowledges support by the Swedish Research Council (VR), the Foundation for Strategic Research (SSF), the Swedish Energy Agency (Energimyndigheten), the European Research Council (Grant No. 854843-FASTCORR) and STandUP. D.T. acknowledges support from the Swedish Research Council (VR) with Grant No. 2019-03666. E.S. acknowledges financial support from the Swedish Research Council (VR) through Grant No. 2017-03832.

[1] C.-K. Chiu, J. C. Y. Teo, A. P. Schnyder, and S. Ryu, Classification of topological quantum matter with symmetries, Rev. Mod. Phys. **88**, 035005 (2016).

[2] M. Johansson, M. Ericsson, E. Sjöqvist, and A. Osterloh, Classification scheme of pure multipartite states based on topological phases, Phys. Rev. A **89**, 012320 (2014).

[3] A. Einstein, B. Podolsky, and N. Rosen, Can quantum-mechanical description of physical reality be considered complete?, Phys. Rev. **47**, 777 (1935).

[4] E. Schrödinger, The present status of quantum mechanics, Naturwissenschaften **23**, 807 (1935).

[5] J. S. Bell, On the Einstein Podolsky Rosen paradox, Physics **1**, 195 (1964).

[6] M. A. Nielsen and I. L. Chuang, *Quantum Computation and Quantum Information*, 10th ed. (Cambridge University Press, Cambridge, UK, 2010).

[7] A. Osterloh, L. Amico, G. Falci, and R. Fazio, Scaling of entanglement close to a quantum phase transition, Nature (London) **416**, 608 (2002).

[8] T. J. Osborne and M. A. Nielsen, Entanglement in a simple quantum phase transition, Phys. Rev. A **66**, 032110 (2002).

[9] T.-C. Wei, D. Das, S. Mukhopadyay, S. Vishveshwara, and P. M. Goldbart, Global entanglement and quantum criticality in spin chains, Phys. Rev. A **71**, 060305(R) (2005).

[10] R. Orús, Universal Geometric Entanglement Close to Quantum Phase Transitions, Phys. Rev. Lett. **100**, 130502 (2008).

[11] W. Son, L. Amico, R. Fazio, A. Hamma, S. Pascazio, and V. Vedral, Quantum phase transition between cluster and antiferromagnetic states, Europhys. Lett. **95**, 50001 (2011).

[12] V. Azimi Mousolou, C. M. Canali, and E. Sjöqvist, Unifying geometric entanglement and geometric phase in a quantum phase transition, Phys. Rev. A **88**, 012310 (2013).

[13] S. Hill and W. K. Wootters, Entanglement of a Pair of Quantum Bits, Phys. Rev. Lett. **78**, 5022 (1997).

[14] W. K. Wootters, Entanglement of Formation of an Arbitrary State of Two Qubits, Phys. Rev. Lett. **80**, 2245 (1998).

[15] M. C. Arnesen, S. Bose, and V. Vedral, Natural Thermal and Magnetic Entanglement in the 1D Heisenberg Model, Phys. Rev. Lett. **87**, 017901 (2001).

[16] M. F. Crommie, C. P. Lutz, D. M. Eigler, Confinement of electrons to quantum corrals on a metal surface, Science **262**, 218 (1993).

[17] L. Mazzola, B. Bellomo, R. Lo Franco, and G. Compagno, Connection among entanglement, mixedness, and nonlocality in a dynamical context, Phys. Rev. A **81**, 052116 (2010).

[18] R. Horodecki, P. Horodecki, and M. Horodecki, Violating Bell inequality by mixed spin-$\frac{1}{2}$ states: Necessary and sufficient condition, Phys. Lett. A **200**, 340 (1995).

[19] B. Horst, K. Bartkiewicz, and A. Miranowicz, Two-qubit mixed states more entangled than pure states: Comparison of the relative entropy of entanglement for a given nonlocality, Phys. Rev. A **87**, 042108 (2013).

[20] G. Vidal and R. F. Werner, Computable measure of entanglement, Phys. Rev. A **65**, 032314 (2002).

[21] A. Miranowicz, A. Grudka, Ordering two-qubit states with concurrence and negativity, Phys. Rev. A **70**, 032326 (2004).

[22] V. Azimi Mousolou, Entanglement fidelity and measure of entanglement, Quant. Info. Proc. **19**, 329 (2020).

[23] Foliation basically means slicing a manifold into equivalence classes of submanifolds [24]. Here, we show that the quantum entanglement foliates the space of coupling parameters into equivalence toric classes.

[24] A. Candel and L. Conlon, Foliations I (Graduate Studies in Mathematics), American Mathematical Society (2000).